Struvite formation associated with the microalgae biofilm matrix of a rotating algal biofilm reactor (RABR) during nutrient removal from municipal wastewater

Kyle M. Hillman and Ronald C. Sims

ABSTRACT

Struvite was observed within the microalgae biofilm matrix of an outdoor, pilot-scale rotating algal biofilm reactor (RABR) designed to remove nitrogen and phosphorus from municipal anaerobic digester filtrate. The bottom layer of cells (2.5-month growth) and two top layers of cells (1-week and 2.5-month growth) were evaluated on east- and west-facing sides of the RABR. Sun orientation and shading effects of upper biofilm layers impacted the species composition and microalgae content of the bottom biofilm layers. Struvite formed within the microalgae biofilm matrix, and a higher struvite content appeared to be correlated with a higher microalgae content. The highest struvite content (expressed as %wt. of total solids) was observed in the east- and west-facing bottom layers of growth and west-facing 1-week growth (5.0%, 4.3%, and 4.1%, respectively). The lowest struvite content was observed in east- and west-facing 2.5-month growth and east-facing 1-week growth (1.1%, 1.5%, and 1.1%, respectively). Despite RABR influent component ion molar ratios with potential for various magnesium and calcium precipitates, microalgae biofilm provided pH and nucleation sites favorable to struvite precipitation. This evaluation is the first in the refereed literature the authors are aware of that reports on the association of struvite formation in the presence of a microalgae biofilm.

Key words | anaerobic digester filtrate, microalgae biofilm, municipal wastewater treatment, nitrogen, phosphorus, struvite

Kyle M. Hillman (corresponding author)
Ronald C. Sims
Biological Engineering Department,
Utah State University,
4105 Old Main Hill, Logan, UT 84322-4105,
USA
E-mail: *kyle.m.hillman@gmail.com*

HIGHLIGHTS

- Struvite precipitation observed within microalgae biofilm matrix of rotating algal biofilm reactor
- Sun orientation and biomass harvesting interval influenced struvite content within biofilm
- Biofilm favored struvite over other magnesium and calcium precipitates
- Biofilm may have provided nucleation sites and favorable pH for struvite precipitation

INTRODUCTION

Central Valley Water Reclamation Facility (CVWRF) is the largest municipal wastewater treatment plant in Utah, USA and must meet the new Technology-Based Phosphorus (P) Effluent Limit of 1.0 mg/L set by the Utah Division of Water Quality (DWQ). Current primary effluent concentrations of P range from 3 to 4 mg/L. A side-stream phosphorus removal system is being implemented to remove nitrogen (N) and P through controlled struvite precipitation. Struvite is a mineral precipitate with equimolar magnesium (Mg), ammonium, and phosphate that forms when these ionic constituents supersaturate under alkaline conditions.

Historically, anaerobic digester effluent is filtered using a belt press and the filtrate is recirculated to the headworks of the facility. Magnesium, ammonium, and phosphate are retained in the system and supersaturate over time, causing nuisance struvite precipitation that clogs belts, pumps, and pipes. Due to the local geography, CVWRF has high influent Mg concentrations that significantly contribute to nuisance struvite precipitation (Waddell *et al.* 2003; Melcer & Lindley 2019).

A pilot-scale rotating algal biofilm reactor (RABR) was implemented to treat anaerobic digester filtrate. A scheme of the RABR is shown in Figure 1. Microalgae biofilm

doi: 10.2166/wst.2020.133

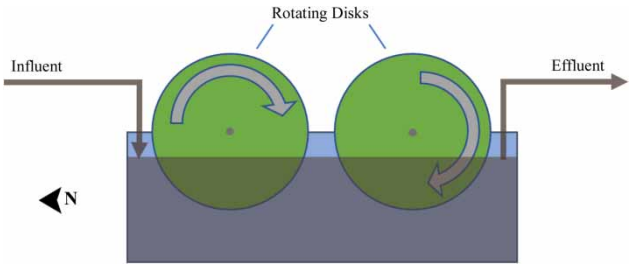

Figure 1 | The CVWRF RABR schematic shows the continuous-flow system. Influent consists of anaerobic digester effluent filtrate and wash water from the belt press used to filter anaerobic digester effluent. Rotating disks covered with microalgae biofilm are 40% submerged in the RABR tank water.

growth removes N and P from wastewater through metabolic activity to form microalgae with the general stoichiometry of $C_{106}N_{16}P_1$ (Sterner & Elser 2002; Cabije *et al.* 2009; Wang *et al.* 2013; Delgadillo-Mirquez *et al.* 2016). Advantages of biofilm-based wastewater treatment systems include low space requirements, reduced hydraulic retention time (HRT), stable performance, low sludge production, and a high concentration of active, diverse biomass that can degrade a range of organic pollutants (Zhao *et al.* 2019). Compared to suspended microalgae growth, biofilm can achieve higher nutrient removal efficiency and biomass is less costly to harvest for subsequent conversion into bioproducts (Christenson & Sims 2012).

RABRs have been used to treat municipal, petrochemical, and produced water (Peterson 2018). N, P, and total suspended solids were reduced by up to 18.1 mg/L (72.4%), 1.00 mg/L (55.6%), and 23.9 mg/L 61.3%) while using a RABR system to treat petrochemical wastewater (Hodges *et al.* 2017). Total dissolved N was reduced from 8.3 mg/L to 1.1 mg/L and total dissolved P was reduced from 4.1 mg/L to 1.1 mg/L while using a RABR system to treat municipal wastewater (Christenson & Sims 2012). RABR technology could help CVWRF meet P effluent standards.

During RABR operation, struvite was observed within the microalgae biofilm matrix. Biofilm-mediated struvite precipitation has engineering implications for enhanced N and P removal from magnesium-rich wastewater. Biomass was harvested on an interval to maintain logarithmic growth and pelletized into fertilizer. Struvite is marketed as a slow-release fertilizer (Szymanska *et al.* 2019). Struvite in the biofilm matrix could enhance fertilizer qualities and marketability of pelletized biomass. The objective of this study was to observe, quantify, and understand struvite formation within microalgae biofilm in the CVWRF RABR system.

MATERIALS AND METHODS

CVWRF RABR

RABR operation started on October 30, 2017. Data for this project were collected June 15, 2019–August 30, 2019, which was after 1 year and 8 months of continuous RABR operation. RABR influent consisted of anaerobic digester effluent filtrate (filtered using a belt press) and belt press wash water. Biofilm was harvested from trickling filters at CVWRF and used as inoculum for the RABR. The RABR operated outdoors under full sun with the disk faces oriented east and west. Table 1 summarizes RABR operational parameters.

Temperature and pH of RABR tank water and biofilm were measured using a Mettler-Toledo FiveGo portable pH and conductivity probe, calibrated daily. Temperature, pH, and samples of biofilm and RABR water were collected between 10 am and 5 pm weekly. Values for pH were converted to hydrogen ion concentration (M) using the equation $pH = -log[H+]$. The hydrogen ion concentration was averaged then converted back to pH using the same equation. Photosynthetically active radiation (PAR) from sunlight was continuously monitored using an LI190R Quantum Sensor (LI-COR) and Campbell Scientific datalogger.

Table 1 | Operating parameters and description of the CVWRF RABR system

RABR parameter	Description
Tank volume	4,500 L (3 m × 1.5 m × 1 m)
Disk arrangement	10 total: 5 disks on each of 2 shafts
Center shafts	2 shafts of 2-inch stainless steel
Disk diameter	1.2 m
Disk rotation speed	~1 revolution per minute (RPM)
HRT	3.6 ± 1.2 hours
Influent to the RABR	Belt press filtrate and wash water
Average influent total Kjeldahl nitrogen concentration[a]	470 mg/L
Average influent phosphorus concentration[a]	24 mg/L
Average influent magnesium concentration[b]	50 mg/L
Average influent calcium concentration[b]	92 mg/L

[a]Average values from CVWRF laboratory, measured four times per month from January to April 2018.
[b]Average values from June 24 and September 30, 2019 measured using ICP-MS.

Struvite observation in the microalgae biofilm matrix

The RABR disks were inoculated with biofilm collected from trickling filters at CVWRF. Light microscope images and species composition of the inoculum is included in the Supplementary Material (Figure A1). There was no struvite in the inoculum.

Three RABR microalgae biofilm harvesting intervals were evaluated: 1-week growth (top layer), 2.5-month growth (top layer), and the bottom layer that developed over a 2.5-month period. The bottom layer was left as inoculum for each growth cycle when the biofilm was harvested weekly. Maintaining a healthy bottom layer of cells is critical for each weekly growth cycle (Gross *et al.* 2015).

Images of the inoculum, biofilm layers, and ash were captured using a light microscope (Leica DM 750) and high-resolution digital camera (Leica ICC 50) to visualize struvite crystals and biofilm species composition. Images of the ash are included in the Supplementary Material (Figure A2). Scanning electron microscopy (SEM) with energy dispersive X-ray spectroscopy (EDS) was performed through the Utah State University Office of Research, Microscopy Core Institute to visualize and confirm struvite crystals in the biofilm.

Nutrient analysis of ash

Total solids (TS) was determined using Method 2540 B, and volatile solids (VS) and ash were determined using Method 2540 E from *Standard Methods* 21st edition (American Public Health Association *et al.* 2005). TS were calculated from initial wet mass. Struvite, diatom cell walls, and other inorganics will remain after volatilization (American Public Health Association *et al.* 2005; Wang & Seibert 2017).

Ash was weighed and collected in a 100 mL volumetric flask. Five millilitres of 1 N sulfuric acid was added to the volumetric flask and swirled to dissolve phosphate precipitates in the ash. Deionized water was added to make a final volume of 100 mL. Sample pH within the volumetric flask was approximately 1 for all samples. Samples were stored at 4 °C but brought to room temperature for analysis.

Struvite is the only potential phosphate precipitate that contains ammonium; thus, ammonium concentration in the ash accurately quantifies struvite concentration in the biofilm (Wang *et al.* 2005; Hao *et al.* 2009). Total nitrogen was measured instead of ammonia because of potential interferences with the ammonia method. Measuring total N is acceptable because ammonium in the struvite is the only N expected in the ash. Organic N was volatilized during ashing. Total nitrogen concentration was measured using HACH Persulfate Digestion HR Test ′N Tube™ (Method 10072). Analysis of variance (ANOVA) was used to determine significance of TS, ash, and struvite content between biofilm layers.

Total P, Mg, and calcium (Ca) were measured using inductively coupled plasma–mass spectroscopy (ICP-MS) by the Utah Water Research Laboratory. Ratios of Mg, Ca, and P in the ash approximates the purity of struvite compared to other potential phosphate precipitates in the biofilm layers.

RESULTS AND DISCUSSION

Temperature and pH of RABR tank water and biofilm

One of the most critical variables in struvite precipitation is pH (Wang *et al.* 2005; Bergmans 2011; Radev *et al.* 2015). RABR water and biofilm pH is shown in Table 2, with an average tank water pH of 7.9 and average biofilm pH of 8.0. There can be 80% P recovery as struvite when pH is 7.9 if the molar concentration of Mg:P is 1.5:1 or greater. Increasing pH in the range of 7.9–8.4 reduces the required Mg:P ratio for struvite precipitation (Esemen *et al.* 2009). Struvite precipitation potential increases exponentially as pH increases in this range (Bergmans 2011). The molar ratio of Mg:Ca:P of settled influent supernatant is 3.8:4.2:1 (46 mg/L Mg, 87 mg/L Ca, and 14 mg/L P), which has potential for both magnesium and calcium phosphate precipitates (Doyle & Parsons 2002; Wang *et al.* 2005).

The optimal pH range for calcium phosphate precipitation is 9–11 (Doyle & Parsons 2002; Song *et al.* 2011), which is above any measured pH in the RABR system (Table 2). Calcium phosphate can precipitate at pH 7.8 if Ca concentration is high and the Mg:Ca ratio is 1:1 or greater (Wang *et al.* 2005), which is characteristic of the RABR influent. However, the pH range and ammonia

Table 2 | Temperature and pH statistics of RABR tank water and microalgae biofilm

		Average	Min	Max	Standard deviation	Coefficient of variation (%)
Tank water	pH	7.9	7.2	8.1	0.23	2.9
	°C	26	21	29	2.2	8.4
Biofilm	pH	8.0	7.9	8.4	0.11	1.3
	°C	25	22	31	2.6	10

availability in the RABR system may favor struvite over calcium phosphate (Song *et al.* 2011).

Although not statistically significant, RABR biofilm pH was measurably higher than water pH. Photosynthesis in microalgae is known to consume carbon dioxide (CO_2) and bicarbonate (HCO_3^-), significantly increasing pH of the growth medium (Craggs *et al.* 2004; Park *et al.* 2011). The same phenomenon is likely to be happening within the biofilm matrix.

At a disk rotation of 1 RPM, the biofilm was continually saturated by RABR water. As such, RABR water may have influenced the pH probe reading of the biofilm. It is possible the pH was significantly higher at the cellular interface than was detected.

RABR microalgae biofilm harvesting interval layers

Different layers and east- vs and west-facing biofilm are expected to have different species composition due to photosensitivity (Sorokin & Krauss 1958; Dodds *et al.* 1999; Roberts *et al.* 2004). PAR values at the CVWRF RABR reached 1,521 $\mu mol \cdot m^{-2} \cdot s^{-1}$ with average maximum daily PAR of 1,348 $\mu mol \cdot m^{-2} \cdot s^{-1}$. Photoinhibition has been observed above PAR values ranging from 100 to 500 $\mu mol \cdot m^{-2} \cdot s^{-1}$ in various microalgae species (Whitelam & Cold 1983; Shyam & Sane 1989; Dodds *et al.* 1999; Roberts *et al.* 2004; Hsieh *et al.* 2014).

The top layers of growth (1-week and 2.5-month) were exposed to direct sunlight. West-facing biofilm had more direct sun exposure with higher intensity because of afternoon sun, while east-facing biofilm only experienced direct sunlight in the morning. The top layers likely consisted of species adapted to higher light intensity, and top cell layers may have had a shading effect on bottom cell layers. The shading effect may have increased photosynthesis and allowed more photosensitive growth in the bottom layers (Dodds *et al.* 1999). New colonization was expected to have high levels of diatoms that would become intermixed within the biofilm matrix as the algal community developed (Roberts *et al.* 2004), which was observed. There could have been more evaporation in the west-facing biofilm due to sun exposure, which could have supersaturated magnesium, ammonium, and phosphate to favor struvite precipitation.

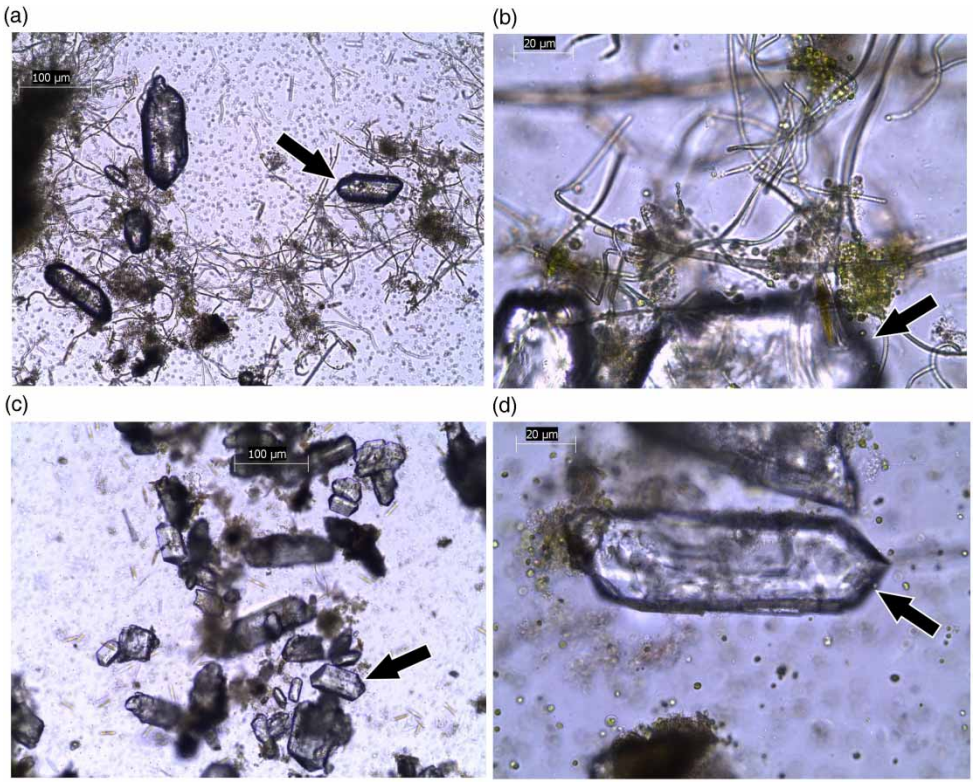

Figure 2 | The bottom layer of the east-facing biofilm magnified at 10× (a) and 40× (b) show *Chlorella*, filamentous microalgae, diatoms, and struvite crystals. Struvite in the east-facing bottom layer appears to be entangled in *Chlorella* and filamentous growth. The bottom layer of the west-facing biofilm at 10× (c) and 40× (d) shows *Chlorella*, diatoms, and struvite crystals. The west-facing bottom layer has no visible filamentous growth, and struvite correlates with *Chlorella*. The black arrows indicate struvite crystals.

Microalgae biofilm bottom layer

The bottom layer of the east-facing biofilm (Figure 2(a) and 2(b)) appeared to have more struvite, *Chlorella*, and filamentous growth than other east-facing layers (Figures 3 and 4). Figure 2 indicates the highest struvite content and most biodiversity in the bottom layer compared to other layers of the east-facing biofilm. The east-facing bottom layer had less diatoms and the most filamentous growth and *Chlorella* compared to other east- and west-facing layers. Struvite crystals appeared to correlate with the presence of various microalgae, but there was no direct correlation with diatoms.

Like the east-facing biofilm, the bottom layer of west-facing biofilm (Figure 2(c) and 2(d)) had more *Chlorella* and filamentous growth with less diatoms than other west-facing layers. The upper layers of the west-facing biofilm may have shaded the bottom layer, which allowed more algal and cyanobacterial growth in the bottom layers. Struvite appeared in higher concentration in the west-facing bottom layer of light microscope images compared to other west-facing layers.

The bottom layers of the east- and west-facing microalgae biofilms had higher apparent struvite and microalgae content than other layers. The bottom layer was shaded by the top layers, which could have reduced photoinhibition of microalgae in the bottom layer. The higher struvite content in the bottom layers could be directly correlated to the favorable biofilm growth conditions and higher microalgae content.

Microalgae biofilm one-week growth

East-facing 1-week growth in Figure 3(a) and 3(b) contains diatoms, *Chlorella*, *Oscillatoria*, and *Pseudoanabaena* (American Public Health Association *et al.* 2005; Komárek & Johansen 2015). East-facing 1-week growth had high struvite content embedded in the biofilm, but clusters of biofilms were sparse. Filamentous microalgae and cyanobacteria, diatoms, and *Chlorella* formed a matrix that appeared to correlate with struvite (Figure 3(b)).

West-facing 1-week growth (Figure 3(c) and 3(d)) also had high struvite content. West-facing 1-week growth had less filamentous growth than east-facing 1-week growth, but struvite appeared to correlate with clusters of *Chlorella* and

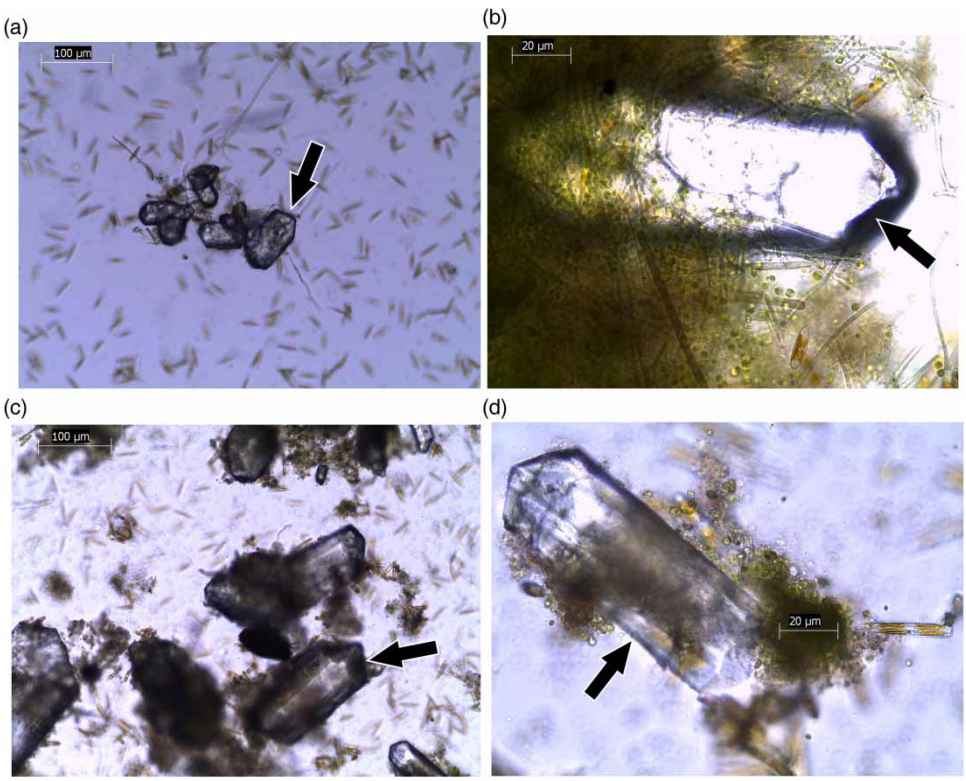

Figure 3 | East-facing 1-week growth magnified at 10× (a) shows struvite crystals attached to strand of filamentous growth and *Chlorella,* while 40× (b) shows struvite crystals embedded in the mixed microalgae biofilm matrix that contains diatoms, *Chlorella*, *Oscillatoria*, and *Pseudoanabaena*. West-facing 1-week growth magnified at 10× (c) and 40× (d) show struvite crystals associated with *Chlorella*. Diatom content appears high in west-facing 1-week growth. Black arrows indicate struvite crystals.

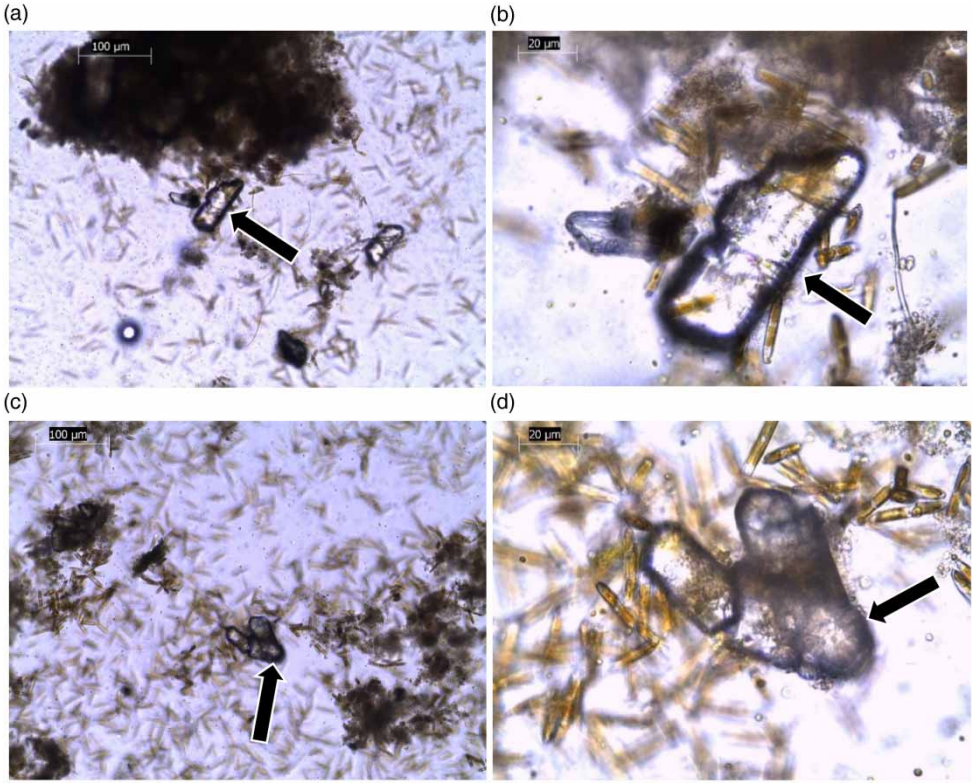

Figure 4 | East-facing 2.5-month growth magnified at 10× (a) and 40× (b) show struvite scattered throughout the biofilm with little filamentous growth or *Chlorella* but abundant brown scum and diatoms. West-facing 2.5-month growth at magnified at 10× (c) and 40× (d) show struvite visible in the brown scum, abundant diatoms, no filamentous growth, and little *Chlorella*. Arrows indicate struvite crystals.

brown scum. Brown scum could be sludge breakthrough from the anaerobic digesters, stained *Chlorella*, or stained biofilm matrix. Filamentous growth was less prevalent in west-facing 1-week growth potentially because the light intensity throughout the day was too high compared to the east-facing biofilm (Whitelam & Cold 1983; Shyam & Sane 1989; Dodds *et al.* 1999; Hsieh *et al.* 2014). *Chlorella* can withstand higher light intensity (Sorokin & Krauss 1958).

Figure 3 shows 1-week growth had a different species composition when east-facing vs west-facing. East-facing 1-week growth experienced direct sunlight only in the early hours of the day while the west-facing experienced direct sunlight throughout the afternoon and evening. East-facing 1-week growth appeared to promote more filamentous growth compared to west-facing. The resulting east-facing biofilm matrix appeared to have high struvite content within the microalgae biofilm matrix.

Microalgae biofilm 2.5-month growth

East-facing 2.5-month growth (Figure 4(a) and 4(b)) mostly consisted of diatoms and brown scum. Struvite, *Chlorella*, and filaments were present at lower concentration than other east-facing biofilm layers. Struvite appeared at lower concentration likely because there was less biofilm matrix to interface with. The high diatom content and low struvite content further indicated a lack of correlation between the presence of diatoms and the presence of struvite.

West-facing 2.5-month growth (Figure 4(c) and 4(d)) was also dominated by diatoms and brown scum. Struvite and *Chlorella* were present in lower quantities than other westcing biofilm layers with no filamentous growth. Photoinhibition from sun exposure may have prevented the development of a biodiverse biofilm with high microalgae content. East- and west-facing 2.5-month growth had similar apparent bioconsortia and struvite content.

SEM/EDS imaging

The use of SEM/EDS verified that struvite is the crystal observed in the light microscopy images in Figures 2–4. Struvite is not the only possible precipitate; calcium and other magnesium precipitates are possible in the measured pH

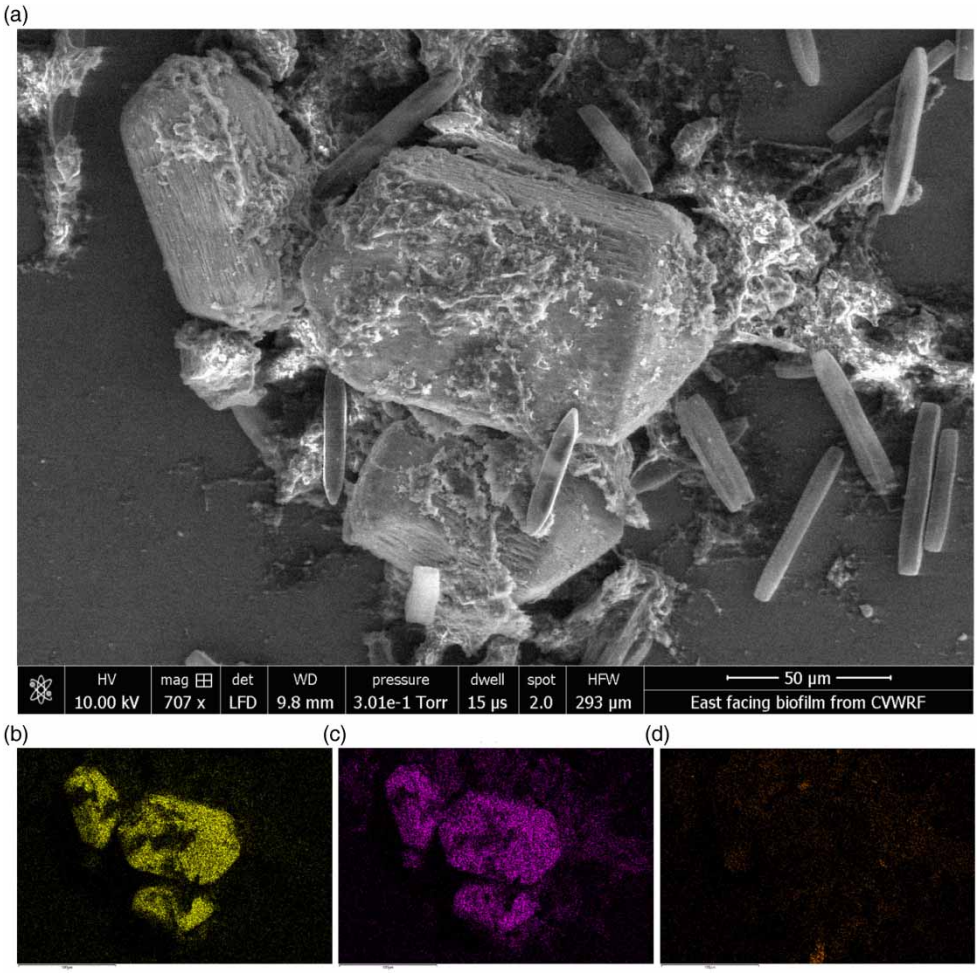

Figure 5 | (a) Struvite crystals from the east-facing biofilm imaged using SEM. The three larger crystals embedded in the biofilm are struvite, while diatoms are the smaller crystal-like forms. Analysis using EDS shows that the atomic signatures of Mg (b), P (c), and Ca (d) in the three large crystals match the Mg:P composition expected in struvite. There is no Ca signature in the three crystals, so they cannot be calcium phosphate.

range of RABR water and biofilm (Doyle & Parsons 2002; Wang *et al.* 2005; Esemen *et al.* 2009; Hao *et al.* 2009). Figure 5(a) shows an SEM image of east-facing RABR biofilm with struvite crystals. Analyzing the crystals using EDS (Figure 5(b)–5(d)) indicated that magnesium and phosphorus were the primary crystal constituents, while calcium was not. Therefore, the crystals in Figures 2–5 are struvite. Additionally, crystals match the expected size and morphology of struvite (Doyle & Parsons 2002; Wang *et al.* 2005).

The map sum spectrum for atomic percentage in Figure 6 further indicates the observed crystals are struvite. P, N, and Mg make up approximately 2.7%, 2.3%, and 2.3%, respectively, of the total atomic density in the SEM image (Figure 5(a)). P, N, and Mg are approximately equimolar, which is expected for struvite.

Nutrient analysis of RABR inoculum and biofilm ash

Ashing the biofilm eliminated organics that may have contained Mg, Ca, N, and P that would have interfered with struvite quantification. Ash consisted mainly of diatom silica cell walls (Gross 2012) and struvite (Figure A2). Struvite content was quantified by measuring total nitrogen in the ash and translating the result to a mass percent of TS, shown in Figure 7. Comparative figures of TS and ash are also included in Figure 7.

The bottom layer of biofilm had significantly higher TS than other layers. The east-facing bottom layer had lower TS and ash than the west-facing bottom layer, but the east-facing bottom layer had significantly more struvite. The higher ash content of the west-facing bottom layer was likely due to diatoms instead of struvite.

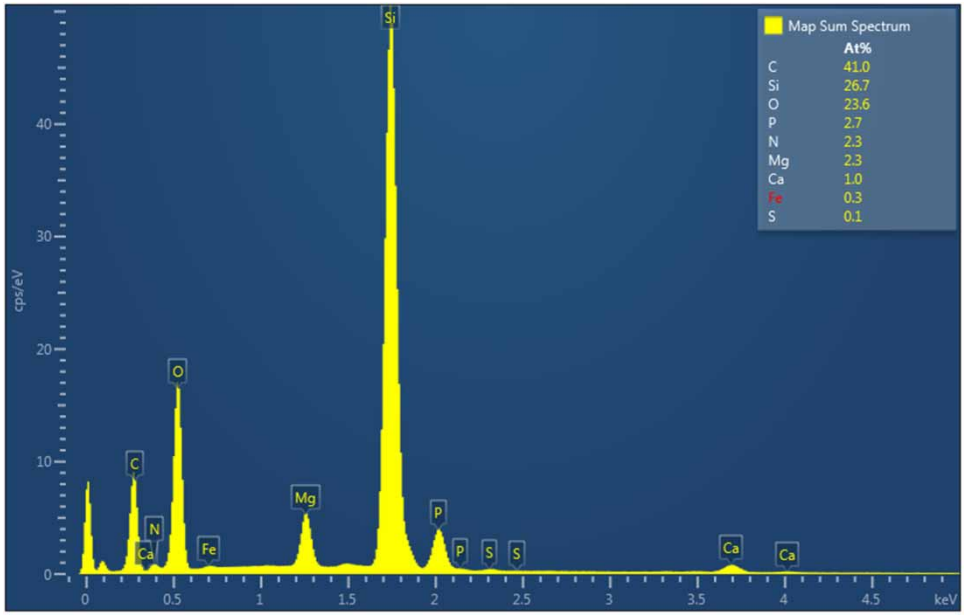

Figure 6 | The map sum spectrum after EDS analysis of the SEM image in Figure 5(a) shows the atomic percentage (At%) of phosphorus (P), nitrogen (N), and magnesium (Mg) are approximately equimolar. Carbon (C), silicon (Si), and oxygen (O) are inaccurate due to environmental interferences and the silica chip the sample was placed on for SEM/EDS.

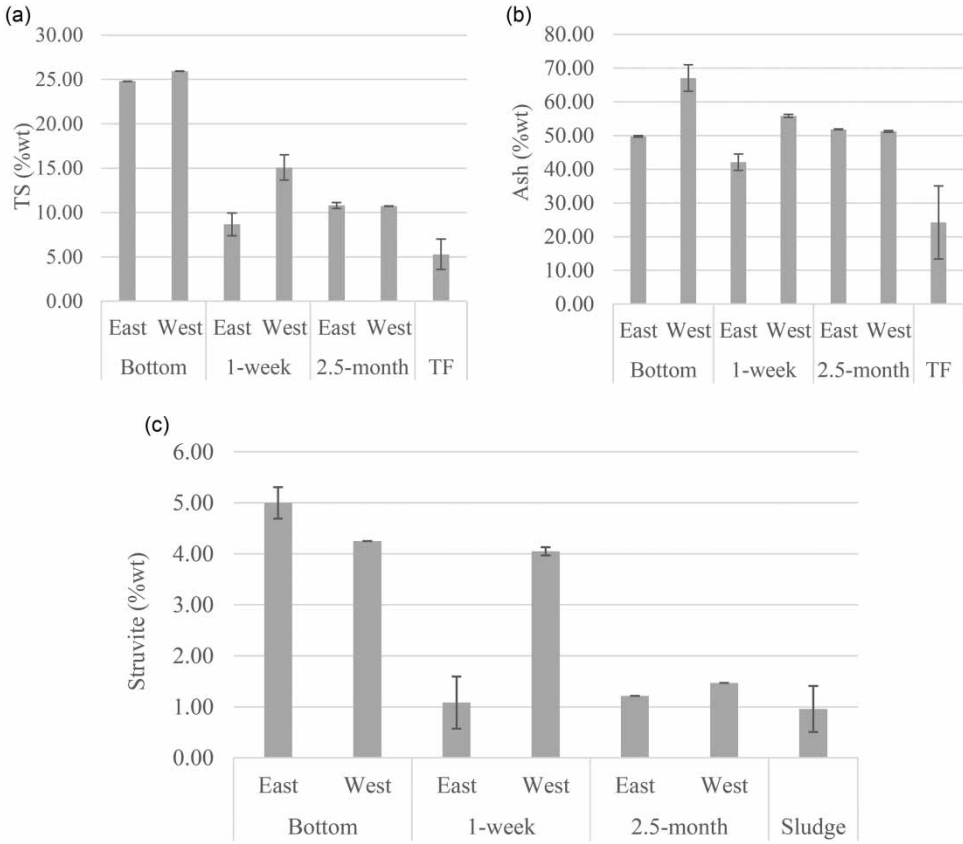

Figure 7 | TS is expressed as percent mass of wet biomass. Ash and struvite are expressed as percent mass of TS. The inoculum is labelled 'TF' for trickling filter. The bottom layer of the biofilm is labeled 'Bottom', 1-week growth labeled '1-week', and 2.5-month growth labeled '2.5 months'.

Struvite content and TS of east-facing 1-week growth was not significantly different from east- or west-facing 2.5-month growth, but significantly lower than the bottom layers. West-facing 1-week growth had significantly more TS, ash, and struvite than east-facing. Struvite content of west-facing 1-week growth was not significantly different from west-facing bottom growth. TS and ash of west-facing 1-week growth was second highest compared to other west-facing layers.

Ash content in east-facing 2.5-month growth was higher than other east-facing layers, likely from diatoms. Struvite and TS of east-facing 2.5-month growth was significantly lower than east-facing bottom growth but not significantly different from east-facing 1-week growth. Struvite, TS, and ash in 2.5-month growth were not significantly different between east- and west-facing. Struvite, TS, and ash were lowest in west-facing 2.5-month growth compared to other west-facing layers.

The highest struvite content on the east-facing disk was in the bottom layer of growth. Figure 3(b) shows struvite embedded in east-facing 1-week biofilm matrix, but Figure 7 indicates east-facing 1-week growth had a similar struvite content to 2.5-month growth. This result was unexpected because 2.5-month growth had a lower microalgae content and more diatoms in the biofilm. Struvite was correlated to and integrated into the microalgae biofilm matrix (Figure 3(b)), so struvite in east-facing 1-week growth may have been low because the biofilm observed in Figure 3(b) may not have had time to develop and spread. The relatively high standard deviation for struvite content in east-facing 1-week growth (Figure 7) could have resulted from non-homogenous samples that consisted of small biofilm clusters with a high struvite content. One week of development may not have been adequate time for the microalgae biofilm clusters to create a uniform biofilm layer like the bottom. The west-facing bottom layer also had a relatively high struvite content.

The highest struvite content on the west-facing disk was 1-week and bottom growth. Figures 2(c), 2(d), 3(c) and 3(d) show west-facing 1-week and bottom growth look similar. Struvite was correlated with *Chlorella*. However, TS and ash were higher in west-facing bottom than 1-week growth. Therefore, TS and ash content were not standalone indicators of struvite content, likely due to diatom influence on TS and ash. Despite the similarity in struvite content, west-facing 1-week and bottom growth had different development times.

Biofilm development time was not the main factor for struvite content in the biofilm. Both the bottom layer and 2.5-month growth developed over a 2.5-month period, but the bottom layer had significantly more struvite than both the east- and west-facing 2.5-month top-layer growth. Additionally, both the west-facing bottom and 1-week growth had relatively high and similar struvite content. Evaporation from sun exposure seems to have had little influence on supersaturation of magnesium, ammonium, and phosphate to precipitate struvite.

Because both 1-week and 2.5-month growth were equally sun-exposed, influences of evaporation and supersaturation should have been similar when in the same sun orientation. Struvite content of east-facing 1-week and 2.5-month growth were not significantly different and received comparable sun exposure because they were the top layers of growth. However, struvite content of the east-facing top layers of growth was significantly lower than the east-facing bottom layer, despite the top layers receiving more sun exposure. If sunlight-induced water evaporation were the main driver of struvite precipitation, expected results would have been opposite.

Additionally, west-facing 1-week and 2.5-month growth received similar sun exposure because they were the top layers of growth, but west-facing 1-week growth had significantly more struvite than west-facing 2.5-month growth. Presence of struvite, therefore, may be more correlated to microalgae than evaporation. Struvite was present in all east- and west-facing biofilm growth layers, but other calcium and magnesium precipitates could also have been present.

According to Figure 8, Mg and Ca molar ratios are consistent with relatively pure struvite in most biofilm layers. For this study, struvite purity is relative to the struvite content vs calcium phosphate in the precipitates. Lower Ca and higher Mg is indicative that the precipitates consist mainly of struvite especially if the Mg/P molar ratio is nearly one (Wang *et al.* 2005).

The inoculum did not contain struvite, but calcium ratios were high. The inoculum contained almost 95% moisture, and the high calcium content in the wastewater may have reacted with phosphate in the liquid phase of inoculum to form calcium phosphate. Biofilm layers with lower TS appeared to have more Ca. Thus, Ca in the ash may have been due to excess wastewater.

The bottom layer had the purest struvite for east- and west-facing biofilm compared to all other layers. The Mg/P molar ratio was nearly one in the east-facing bottom layer, so the Ca present in the bottom layer may have been the baseline Ca in the biofilm or wastewater.

Calcium precipitates may have been present at low quantities in east-facing 1-week growth, but Ca was not

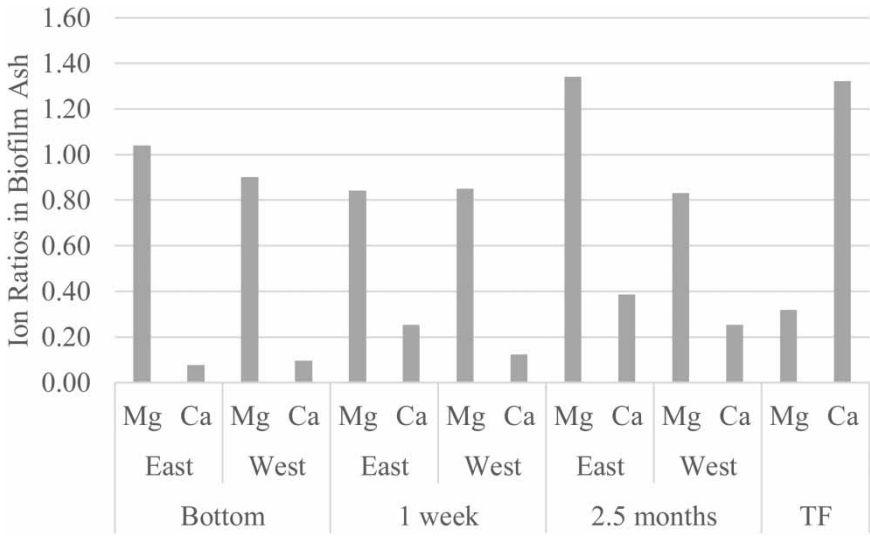

Figure 8 | ICP-MS results for relative Mg and Ca molar ratios normalized to P represent the relative purity of struvite vs calcium phosphate in biofilm precipitates. The biofilm inoculum (TF) does not contain struvite.

above baseline levels in west-facing 1-week growth. The precipitates in 1-week growth were mostly consistent with pure struvite.

Struvite purity decreased in east-facing 2.5-month growth. Precipitates had an excess of over 0.3 moles of P per mole of Mg. Excess P was likely attributable to calcium phosphate as there was higher calcium in east-facing 2.5-month growth. Molar ratios for Mg and Ca were similar for west-facing 2.5-month growth and east-facing 1-week growth. Most of the P in west-facing 2.5-month and east-facing 1-week growth was likely from struvite, but some calcium phosphate may have been present.

Despite the influent Mg:Ca:P molar concentration having potential for both struvite and calcium phosphate precipitation, the biofilm favored struvite precipitation. The biofilm mechanism that favored struvite over calcium phosphate formation was likely pH regulation while providing nucleation sites for struvite seed crystals. Presence of struvite seed crystals or attachment surfaces significantly reduces nucleation induction time for struvite formation (Doyle & Parsons 2002; Agrawal *et al.* 2018).

CONCLUSIONS

While utilizing an RABR system for nutrient removal from municipal anaerobic digester effluent filtrate, struvite was observed in the microalgae biofilm. This evaluation is the first in the refereed literature the authors are aware of that reports on the association of struvite formation with the presence of microalgae biofilm. Component ion molar ratios of Ca, Mg, and P favor both struvite and calcium phosphate precipitation, but the microalgae biofilm favored struvite, likely due to pH regulation, nucleation surfaces, and the high ammonia content in municipal wastewater. Struvite was quantified in three east-facing and west-facing growth development layers of microalgae biofilm.

The highest struvite content was observed in the bottom layer of the east-facing biofilm and could have been correlated to the higher microalgae content in that layer. Photoinhibition and shading may have influenced bioconsortia in the various layers, which may explain differences in struvite content. Struvite did not seem to be directly correlated to TS, ash content, diatom content, biofilm development time, or sun-induced water evaporation alone, but all may have been factors. Struvite appeared to be directly correlated with the microalgae biofilm matrix.

More research is needed to determine the exact mechanism of struvite formation in the microalgae biofilm matrix. Measuring the pH gradient through different biofilm layers and at the cellular interface within the biofilm matrix may elucidate struvite formation potential in different layers. A detailed species composition of struvite-containing, mixed microalgae biofilm may determine if certain species are more correlated to struvite precipitation. To quantify struvite correlation with a higher microalgae content, photosynthetic activity and chlorophyll concentration should be compared to relative struvite content. Optimization of struvite production could be evaluated through biofilm development times, PAR, and disk RPM. Multiple RABR

systems connected in series or a synthetic wastewater experiment may clarify required molar concentrations of Mg, Ca, P, and ammonia for struvite formation in mixed microalgae biofilms.

ACKNOWLEDGEMENTS

This project was made possible with funding from the Huntsman Environmental Research Center and research facilities provided by the Sustainable Waste to Bioproducts Engineering Center. Thanks to WesTech Engineering, Inc. for construction of the pilot-scale rotating algal biofilm reactor. Thanks to Central Valley Water Reclamation Facility – specifically to Dr Phil Heck for the first observation of struvite on the RABR, for collaboration to test the RABR on anaerobic digester effluent, and for adding valuable content to the introduction. Thank you to Dr FenAnn Shen with the Utah State University Office of Research, Microscopy Core Institute for SEM/EDS imaging. Thank you to Joshua Hortin with the Utah Water Research Laboratory for Mg, Ca, and P analysis via ICP-MS. Thank you to Nathan Guymon for PAR data collection at the CVWRF RABR. Thank you to Dylan Ellis, Jacob Watkins, Steven White, and Taylor Adams for invaluable laboratory assistance and long days in the field. Special thanks to Dr Ronald Sims for guidance and mentorship every step of the way.

SUPPLEMENTARY MATERIAL

The Supplementary Material for this paper is available online at https://dx.doi.org/10.2166/wst.2020.133.

REFERENCES

Agrawal, S., Guest, J. S. & Cusick, R. D. (2018). Elucidating the impacts of initial supersaturation and seed crystal loading on struvite precipitation kinetics, fines production, and crystal growth. *Water Research* **132**, 252–259. https://doi.org/10.1016/J.WATRES.2018.01.002

American Public Health Association, American Water Works Association, & Water Environment Federation 2005 *Standard Methods for the Examination of Water and Wastewater*, 21st edn (A. D. Eaton, M. A. H. Franson, L. S. Clesceri, E. W. Rice & A. E. Greenberg, eds). American Public Health Association, Washington, DC. Available from: https://books.google.com/books/about/Standard_Methods_for_the_Examination_of.html?id=buTn1rmfSI4C.

Bergmans, B. 2011 *Struvite Recovery From Digested Sludge At WWTP West*. Delft University of Technology. Available from: www.drinkwater.tudelft.nl.

Cabije, A. H., Agapay, R. C. & Tampus, M. V. 2009 Carbon-nitrogen-phosphorus removal and biofilm growth characteristics in an integrated wastewater treatment system involving a rotating biological contactor. *Asia-Pacific Journal of Chemical Engineering* **4** (5), 735–743. https://doi.org/10.1002/apj.329.

Christenson, L. B. & Sims, R. C. 2012 Rotating algal biofilm reactor and spool harvester for wastewater treatment with biofuels by-products. *Biotechnology and Bioengineering* **109** (7), 1674–1684. https://doi.org/10.1002/bit.24451.

Craggs, R. J., Sukias, J. P., Tanner, C. T. & Davies-Colley, R. J. 2004 Advanced pond system for dairy-farm effluent treatment. *New Zealand Journal of Agricultural Research* **47** (449), 449–460. https://doi.org/10.1080/00288233.2004.9513613.

Delgadillo-Mirquez, L., Lopes, F., Taidi, B. & Pareau, D. 2016 Nitrogen and phosphate removal from wastewater with a mixed microalgae and bacteria culture. *Biotechnology Reports* **11**, 18–26. https://doi.org/10.1016/j.btre.2016.04.003.

Dodds, W. K., Biggs, B. J. F. & Lowe, R. L. 1999 Photosynthesis-irradiance patterns in benthic microalgae: variations as a function of assemblage thickness and community structure. *Journal of Phycology* **35** (1), 42–53. https://doi.org/10.1046/j.1529-8817.1999.3510042.x.

Doyle, J. D. & Parsons, S. A. 2002 Struvite formation, control and recovery. *Water Research* **36** (16), 3925–3940. https://doi.org/10.1016/S0043-1354(02)00126-4.

Esemen, T., Rand, W., Dockhorn, T. & Dichtl, N. 2009 Increasing cost efficiency of struvite precipitation by using alternative precipitants and P-remobilization from sewage sludge. In: *International Conference on Nutrient Recovery From Wastewater Streams* (K. Ashley, D. Mavinic & F. Koch, eds). IWA Publishing, Vancouver, pp. 269–331. Available from: https://books.google.com/books?hl=en&lr=&id=3gM5ixYKYFIC&oi=fnd&pg=PA79&dq=a+quantitative+method+analyzing+the+content+of+struvite+in+phosphate-based+precipitates&ots=17NmOi0-Ol&sig=HKRQidKTgc9pJFdalGrB6G5OMDI#v=onepage&q&f=false.

Gross, M. 2012 The mysteries of the diatoms. *Current Biology* **22** (15), R581–R585. https://doi.org/10.1016/J.CUB.2012.07.041.

Gross, M., Jarboe, D. & Wen, Z. 2015 Biofilm-based algal cultivation systems. *Applied Microbiology and Biotechnology* **99** (14), 5781–5789. https://doi.org/10.1007/s00253-015-6736-5.

Hao, X.-D., Wang, C.-C., Lan, L. & van Loosdrecht, M. C. M. 2009 A quantitative method analyzing the content of struvite in phosphate-based precipitates. In: *International Conference on Nutrient Recovery From Wastewater Streams*. IWA Publishing, Vancouver, pp. 79–88. Available from: https://books.google.com/books?hl=en&lr=&id=3gM5ixYKYFIC&oi=fnd&pg=PA79&dq=a+quantitative+method+analyzing+the+content+of+struvite+in+phosphate-based+precipitates&ots=17NmOi0-Ol&sig=HKRQidKTgc9pJFdalGrB6G5OMDI#v=onepage&q=a quantitative method analy.

Hodges, A., Fica, Z., Wanlass, J., VanDarlin, J. & Sims, R. 2017 Nutrient and suspended solids removal from petrochemical wastewater via microalgal biofilm cultivation. *Chemosphere* **174**, 46–48. https://doi.org/10.1016/j.chemosphere.2017.01.107.

Hsieh, P., Pedersen, J. Z. & Bruno, L. 2014 Photoinhibition of cyanobacteria and its application in cultural heritage conservation. *Photochemistry and Photobiology* **90** (3), 533–543. https://doi.org/10.1111/php.12208.

Komárek, J. & Johansen, J. R. 2015 Filamentous cyanobacteria. In: *Freshwater Algae of North America*, 2nd edn (J. D. Wehr, R. G. Sheath & J. P. Kociolek, eds). Academic Press, pp. 135–235. Available from: https://doi.org/10.1016/B978-0-12-385876-4.00004-9.

Melcer, H. & Lindley, T. 2019 *CVWRF Side Stream Phosphorus Removal Analysis, v.4. Draft Memorandum Prepared for Central Valley Water Reclamation Facility*. Unpublished Draft Memorandum Prepared by Brown and Caldwell, Midvale.

Park, J. B. K., Craggs, R. J. & Shilton, A. N. 2011 Wastewater treatment high rate algal ponds for biofuel production. *Bioresource Technology* **102** (1), 35–42. https://doi.org/10.1016/J.BIORTECH.2010.06.158.

Peterson, B. L. 2018 *Development and optimization of a produced water, biofilm based microalgae cultivation system for biocrude conversion using hydrothermal liquefaction*. All Graduate Theses and Dissertations. Utah State University, Logan. https://digitalcommons.usu.edu/etd/7237/.

Radev, D., Peeva, G. & Nenov, V. 2015 pH control during the struvite precipitation process of wastewaters. *Wastewaters. Journal of Water Resource and Protection* **7**, 1399–1408. https://doi.org/10.4236/jwarp.2015.716113.

Roberts, S., Sabater, S. & Beardall, J. 2004 Benthic microalgal colonization in streams of differing riparian cover and light availability. *Journal of Phycology* **40** (6), 1004–1012. https://doi.org/10.1111/j.1529-8817.2004.03333.x.

Shyam, R. & Sane, P. V. 1989 Photoinhibition of photosynthesis and its recovery in low and high light acclimatized blue-green algae (Cyanobacteria) *Spirulina platensis*. *Biochemie Und Physiologie Der Pflanzen* **185** (3–4), 211–219. https://doi.org/10.1016/s0015-3796(89)80083-6.

Song, Y.-H., Qiu, G.-L., Yuan, P., Cui, X.-Y., Peng, J.-F., Zeng, P., Duan, L., Xiang, L.-C. & Qian, F. 2011 Nutrients removal and recovery from anaerobically digested swine wastewater by struvite crystallization without chemical additions. *Journal of Hazardous Materials* **190** (1–3), 140–149. https://doi.org/10.1016/J.JHAZMAT.2011.03.015.

Sorokin, C. & Krauss, R. W. 1958 The effects of light intensity on the growth rates of green algae. *Plant Physiology* **33** (2), 109–113. https://doi.org/10.1104/pp.33.2.109.

Sterner, R. W. & Elser, J. J. 2002 *Ecological Stoichiometry: The Biology of Elements From Molecules to the Bioshphere*, 1st edn. Princeton University Press, Princeton. Available from: https://books.google.com/books?id=BWjVDQAAQBAJ&pg=PA28&lpg=PA28&dq=C106+N16+P1&source=bl&ots=U7Dmvttc-I&sig=ACfU3U0uo26lez_JXggioHK86mSqdo4U9A&hl=en&sa=X&ved=2ahUKEwiPt5Gbw9bmAhWVHTQIHRmVC6sQ6AEwAXoECAoQAQ#v=onepage&q=C106 N16 P1&f=false.

Szymanska, M., Szara, E., Was, A., Sosulski, T., Van Pruissen, G. W. P. & Cornelissen, R. L. 2019 Struvite – an innovative fertilizer from anaerobic digestate produced in a bio-refinery. *Energies* **12** (2), 1–9. https://doi.org/10.3390/en12020296.

Waddell, K. M., Gerner, S. J., Thiros, S. A., Giddings, E. M., Baskin, R. L., Cederberg, J. R. & Albano, C. M. 2003 *Water Quality in the Great Salt Lake Basins, Utah, Idaho, and Wyoming, 1998–2001*. Available from: http://ut.water.usgs.gov/nawqa/.

Wang, J., Burken, J. G., Zhang, X. (J.) & Surampalli, R. 2005 Engineered struvite precipitation: impacts of component-ion molar ratios and pH. *Journal of Environmental Engineering* **131** (10), 1433–1440. https://doi.org/10.1061/(ASCE)0733-9372(2005)131:10(1433).

Wang, J.-K. & Seibert, M. 2017 Prospects for commercial production of diatoms. *Biotechnology for Biofuels* **10** (16). https://doi.org/10.1186/s13068-017-0699-y.

Wang, C., Yu, X., Lv, H. & Yang, J. 2013 Nitrogen and phosphorus removal from municipal wastewater by the green alga *Chlorella* sp. *Journal of Environmental Biology* **34** (SUPPL.2), 421–425.

Whitelam, G. C. & Cold, G. A. 1983 Photoinhibition of photosynthesis in the cyanobacterium *Microcystis aeruginosa*. *Planta* **157** (6), 561–566. https://doi.org/10.1007/BF00396889.

Zhao, Y., Liu, D., Huang, W., Yang, Y., Ji, M., Nghiem, L. D., Trinh, Q. T. & Tran, N. H. 2019 Insights into biofilm carriers for biological wastewater treatment processes: current state-of-the-art, challenges, and opportunities. *Bioresource Technology* **288**, 121619. https://doi.org/10.1016/j.biortech.2019.121619.

First received 21 November 2019; accepted in revised form 29 February 2020. Available online 26 March 2020